JOURNAL OF MATERIALS SCIENCE 11 (1976) 2027–2035

Hydroxylapatite synthesis and characterization in dense polycrystalline form

M. JARCHO, C. H. BOLEN
Sterling-Winthrop Research Institute, Division of Sterling Drug, Inc, Rensselaer, New York, USA

M. B. THOMAS, J. BOBICK, J. F. KAY, R. H. DOREMUS
Materials Engineering Department, Rensselaer Polytechnic Institute, Troy, New York, USA

A new process is described for preparing dense, polycrystalline hydroxylapatite. This material has close to theoretical density and is free of fine pores and second phases. The best material has an average compressive strength of 917 MN m^{-2} (133 × 10^3 psi), and polished samples have an average tensile strength of 196 MN m^{-2} (28.4 × 10^3 psi). The material is highly translucent, and the degree of translucence depends upon processing conditions. The relationship between processing variables and microstructure, strength, and translucence is described. This dense hydroxylapatite has good promise for bone implants and dental applications.

1. Introduction

Hydroxylapatite is a particularly attractive material for bone and tooth implants since it closely resembles vertebrate tooth and bone mineral and has proven to be biologically compatible with these tissues [1, 2]. Previous attempts to prepare strong forms of hydroxylapatite and related calcium phosphates have ranged from conventional powder compaction-sintering techniques [3–5] to a hydrothermal exchange process in which marine coral is converted to a hydroxylapatite replica [6]. The principal limitation of these materials is that they are weak and often contain other crystalline phases and many fine pores. This paper describes a new process for forming a dense polycrystalline hydroxylapatite that is substantially stronger than other hydroxylapatite materials [7]. This material elicits an excellent biological response when implanted in bone [2], and because of its high degree of translucence, it also has potential for use in aesthetic restorative and preventive dental applications [7]. Various experimental techniques were used to characterize the hydroxylapatite: microstructural, mechanical, and optical properties were emphasized.

2. Experimental methods

2.1. X-ray diffraction

Solid samples were crushed to fine powder and examined in a Norelco diffractometer with copper $K\alpha$ radiation and a scan rate of 0.5° min^{-1}. The recorded peaks were compared with the ASTM powder diffraction file; there was good agreement between our samples and ASTM data for hydroxylapatite ($Ca_{10}(PO_4)_6(OH)_2$). In some samples peaks for α or β whitlockite ($Ca_3(PO_4)_2$) were also identified.

The relative amounts of various phases in the fired samples were calculated from the integrated intensities P of selected reflections of the phases. In a two-phase mixture:

$$\frac{P_1}{P_1^0} = \frac{w_1 M_1}{w_1(M_1 - M_2) + M_2} \quad (1)$$

where P_1^0 is the integrated intensity from pure phase 1, P_1 is from the sample being examined, w_1 is the weight fraction of phase 1, and M_1 and M_2 are mass absorption coefficients. The mass absorption coefficients for apatite and whitlockite were calculated to be 87.38 and 97.08, respectively.

The peaks used in the calculations were: apatite (3 0 0); α-whitlockite (4 0 2), (4 4 1), and (5 1 1) combined, and β-whitlockite (0, 2, 1 0).

2.2. Electron microscopy

Two-stage replicas were made by shadowing a collodion replica of the sample surface with chromium and then coating it with carbon. The replicas were examined in a Hitachi HU-11B microscope at 100 or 125 kV. Fracture surfaces of apatite samples were initally etched in 1 to 4% hydrofluoric acid to reveal the grain structure. However, the HF sometimes gave areas on the crystal surface covered with small crystals, probably calcium fluoride [8]. Other solutions (1% HNO_3, 0.12M EDTA, and 0.15M lactic acid, pH 2.4) were tried, and the lactic acid proved to best reveal the hydroxylapatite microstructure. Thus a 10 min lactic acid etch was used in subsequent work. It was also possible to observe the microstructure without etching in some samples.

Some samples were thinned with a Commonwealth Science Corp IMMI III ion thinner for direct observation in transmission. Electron diffraction studies were also possible on these thinned samples.

An extraction technique was used to observe the fine crystals in the dried filter cake. The Bioden film used for the replica was soaked in methyl acetate and placed on the surface of the cake. After the film dried it was slowly peeled off, extracting a thin layer of the cake. Then a thin film carbon was deposited on to the extracted layer, and the layer was placed on a sample grid with the Bioden film facing the grid. The backing film was washed away with methyl acetate, leaving the cake layer on the carbon film for observation in the microscope.

Grain size and pore fractions were estimated from the micrographs. The average grain size, D, was determined by the linear intercept method [9], using circles 4 and 5 cm in diameter and the equation $D = c/NM$, where c is circle diameter, N the number of intersections with grain boundaries, and M the magnification of the micrograph.

The volume fraction of pores was determined by the grid method [10]. The fraction of grid points that lie on pores in the micrograph was taken as the volume fraction of pores.

Density measurements were made by the displacement method using doubly distilled water.

2.3. Reflectivity measurements

Flat samples of 2 to 3 cm^2 were ground to uniform thickness (1 to 2 mm) with abrasive paper and both sides polished to a 1 μm finish with diamond paste. The reflectance was measured with a KCS-40 double-beam spectrophotometer with an integrating sphere. Packed $BaSO_4$ powder was used as a white standard. The sample was mounted on a black tile background with a thin layer of oil of the same refractive index as the sample. More experimental details and interpretations of the results in terms of transmittance and scattering of the samples are described elsewhere [11].

2.4. Strength measurements

Bars of the polycrystalline hydroxylapatite of dimension 0.2 cm x 0.2 cm x 3 cm were cut from plates with a diamond saw. Some bars were etched and polsihed before testing. Most tests were in three-point bending; a few tests in four-point bending gave similar results. An Instron testing unit was used at various cross-head speeds. Compression tests were made on cylinders about 2.0 mm high and 4.6 mm diameter. Two of these cylinders stacked one on top of the other gave the same average compression strengths as a single cylinder. More results and experimental details are given in [12].

Knoop hardness tests were made with a diamond indentor; each sample was indented 20 times with a 200 g load.

2.5. Electrical conductivity

Silver paste electrodes were dried on to flat samples of the hydroxylapatite, and the conductivity measured with a Keithly 601 electrometer as a function of temperature.

2.6. Chemical analysis

Standard EDTA titration techniques were used for calcium analysis. Phosphate was determined spectrophotometrically by the method of Murphy and Riley [13]. The estimated error in Ca/PO_4 is $\pm$ 2%.

3. Process of forming polycrystalline hydroxylapatite

The precipitation of hydroxylapatite crystals was based on that previously established [14], with some modifications.

Reagent grade $Ca(NO_3)_2 \cdot 4H_2O$ and $(NH_4)_2$

HPO_4 were dispensed from concentrated stock solutions which had been doubly analysed for Ca^{2+} and PO_4^{3-}. Contact with metals by the reaction mixture and the wet filter cake was avoided since the presence of extraneous metal ions can color the ceramic. Although rigorous exclusion of CO_2 from the reaction mixture was apparently not required, unnecessary contact with air should be avoided.

A solution of $Ca(NO_3)_2$ (1.00 M) in 900 ml distilled water was brought to pH 11 to 12 with concentrated NH_4OH ($\approx$ 30 ml) and thereafter diluted to 1800 ml. A solution of $(NH_4)_2HPO_4$ (0.600 M) in 1500 ml distilled water was brought to pH $\approx$ 11 to 12 with concentrated NH_4OH ($\approx$ 750 ml) and thereafter diluted to 3200 ml to dissolve the resulting precipitate. The pH was again checked and additional concentrated NH_4OH was added if necessary.

The calcium solution was vigorously stirred at room temperature, and the phosphate solution was added dropwise over 30 to 40 min to produce a milky, somewhat gelatinous precipitate which was then stirred and/or boiled for different periods of time (see Section 4). The reaction mixture was then centrifuged (2000 rpm for 10 min) and the precipitate thoroughly washed with distilled water and recentrifuged. The resulting sludge was homogeneously suspended in distilled water and filtered on a Büchner funnel (25 cm) with application of mild suction and a rubber dam. After filtration for several hours, the compact, sticky filter cake was dried at 90° C for 15 h. In this preliminary forming process, shrinkage and cracking took place during the drying period, but large plates ($\approx$ 3 mm thick) of compact material, with surface dimensions ranging up to 100 cm^2, were obtained. The yield of hydroxylapatite compact was 90 to 100 g.

Sintering was carried out at 1000 to 1200° C for 1 h to produce dense polycrystalline hydroxylapatite. Samples were put in a cold furnace which took about 1 h to heat to sintering temperature, and were cooled in the furnace after sintering.

Certain steps in the process were found to influence critically the microstructure and properties of the sintered ceramic; these effects are discussed in the results section.

4. Experimental results

4.1. Composition

Observed X-ray diffraction peaks in the fired material correlated closely with ASTM data for hydroxylapatite. Peaks for α- and β-whitlockite ($Ca_3(PO_4)_2$) were also observed in some samples. The presence of α- and β-whitlockite in the sintered ceramic depended mainly on the composition of the precipitated crystals, as detailed below.

X-ray diffraction from the filtered crystals before firing showed only a few broad peaks corresponding to peaks of highest intensity in the sintered material. Thus the filtered crystals were mainly hydroxylapatite, but were very small, with the size estimated [15] from the peak broadening to be less than about 300 Å. This result agrees with microscopy reported below.

The effects of processing variables on the composition of the filtered crystals and on the composition of the fired ceramic are given in Table I. The most important factor is the time that the mixture of initial precipitate and supernatant liquor is stirred before it is centrifuged. Stirring times of 24 h or greater invariably give a Ca/P ratio

TABLE I Composition of filtered crystals and hydroxylapatite as fired at 1100° C for 1 h as a function of stirring time

Sample no.	Stirring time (h)	Chemical anslysis before firing (wt %)			Phase composition of fired crystals (wt %)			Translucence grading
		Ca	P	Ca/P	Apatite	α-whit.	β-whit.	
$Ca_{10}(PO_4)_6(OH)_2$		39.90	18.50	1.667				
Q–1	1/12	36.6	18.2	1.55	23		77	6
Q–2	3/4				25		75	6
Q–3	2	36.6	18.0	1.57	39		61	6
Q–4	$4\frac{1}{2}$				98	2		5
Q–5	7	37.0	17.0	1.68	98	2		5
Q–6	7 Plus 17 h standing	37.2	17.0	1.69	100	0	0	2
Q–7	24	37.4	17.1	1.69	100	0	0	1
Q–8	48	37.4	16.8	1.72	100	0	0	2
R–1	48	36.6	17.1	1.65	100	0	0	2

very close to the correct apatite stoichiometry (Ca/P = 1.67) in the precipitate, and 100% apatite in the fired ceramic. These results are consistent with those of Eanes *et al.* [16], who showed that precipitates from alkaline calcium phosphate solutions must be held for more than 7 h at 25° C to convert them completely to the hydroxylapatite composition (Ca/P ratio of 1.67). This conversion reaction is considered further in the discussion section.

The composition of the crystals fired 1 h at 1100° C depended on the composition of the precipitated crystals. If the latter had Ca/P ratios corresponding to the correct apatite stoichiometry of 1.67, the fired ceramic was 100% apatite from the X-ray measurements. The limit of detection of the X-ray measurements was about 0.5 wt% of a phase; nevertheless these results were confirmed by the microstructural examination reported below, in which a considerably smaller phase fraction can be observed. The ratio of calcium to phosphorous in the initial solutions must of course be 1.67 to insure that the precipitated crystals attain this ratio.

The results of Table I were confirmed by a number of other experiments in which other factors in the precipitation process were varied, such as the temperature during stirring and the time of standing after centrifugation. A correlation between composition of the precipitate and the fired ceramic was always found. As has been previously reported by others [16], the maturation of the apatite precipitate was temperature dependent, thus boiling the reaction mixture for about 1 h appeared to be equivalent to stirring overnight at 25° C.

The translucence of each fired sample was visually graded from 1 (most translucent) to 7 (most opaque) as reported in Table I. Samples containing second phases were much more opaque than samples without these phases.

If the precipitated crystals had the correct hydroxylapatite stoichiometry the fired ceramic contained 100% hydroxylapatite by X-ray measurments for firing temperatures up to 1200° C (1 h firing time).

4.2. Microstructure

Electron micrographs of extractions replicas of precipitated crystals in the filter cake are shown in Figs. 1 and 2. Agglomerates of crystals are visible, and the individual crystals are apparently of dimension about 200 Å. Estimates of crystal size from X-ray line-broadening for the same samples gives about 200 Å from the (2 2 2) reflection and about 350 Å from the (0 0 2).

Microstructural results for a number of different fired samples are summarized in Table II. Attention is first focused on the C series of samples, which were fired from precipitated crystals with correct hydroxylapatite stoichiometry. From X-ray analysis, all the fired samples were found to contain 100% apatite. Samples C–7 fired at 950° C (Fig. 3) showed large pores, low density, opacity, and many fine particles (≈ 0.1 μm in size), indicating incomplete sintering. The sample fired at 1000° C (Fig. 4) showed no pores in the micrograph and good translucence, indicating that sintering was complete at this temperature. The most translucent samples were obtained after firing at 1100° C (Fig. 5); considerable grain growth occurred compared to the sample fired at 1000° C, indicating that there was some light scattering from the grain boundaries. The density

TABLE II Microstructure, density, and translucence for polycrystalline hydroxylapatite

Sample no.	Firing temp. (° C)	Average grain size (μm)	Volume fraction of pores	Density % theoretical	Scattering ceofficient at 500 nm (cm^{-1})	Translucence grading	wt % apatite from X-rays
Q–3	1100	0.601	0	–		6	39
Q–4	1100	0.448	0.018	–		5	98
Q–5	1100	0.472	0.016	–		5	98
E–9	1150	0.536	0.031	96.5	30.0	6	60
F–67	1200	0.363	0.043	90.7		7	86
C–7	950	–	0.15			7	100
C–2	1000	0.151	0	–		2	100
C–6	1100	0.284	0	99.6	8.4	1	100
C–8	1150	0.628	0	–	10.4	3	100
C–5	1190	0.712	0	99.4	14.8	4	100
D–8	1150	–	0	–	13.2	3	100

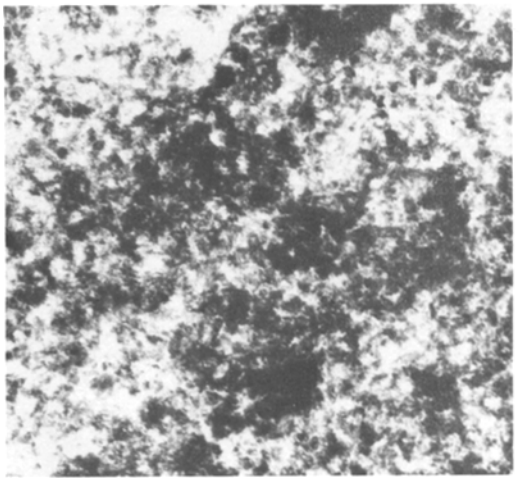

Figure 1 Electron micrograph from extraction replica of precititated hydroxylapatite crystals in the filter cake, sample N–27, × 57 500.

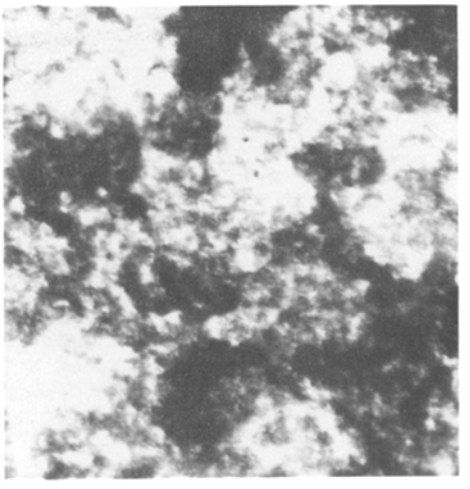

Figure 2 Electron micrograph from extraction replica of precipitated hydroxylapatite crystals in the filter cake, sample N–32, × 57 500.

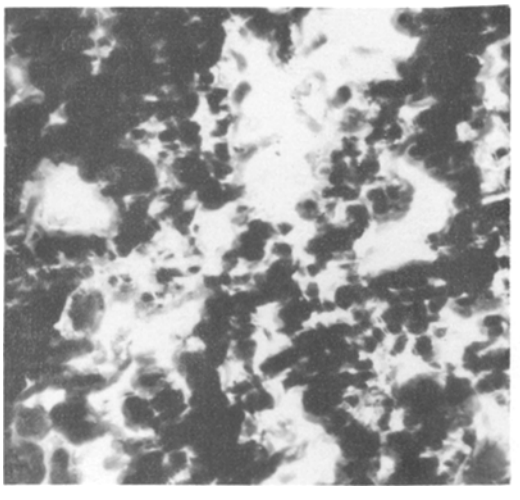

Figure 3 Electron micrograph from two-stage replica of hydroxylapatite fired 1 h at 950° C (C–7), × 33 000.

Figure 4 Electron micrograph from two-stage replica of hydroxylapatite fired 1 h at 1000° C (C–2), × 33 000.

of the sample fired at 1100° C was 3.143 g cm^{-3} or probably within experimental error of the theoretical density of 3.156. There is some evidence for exaggerated grain growth (secondary recrystallization) in Fig. 5, which becomes more marked at higher firing temperatures. Samples fired at higher temperatures (Figs. 6 and 7) show increasing grain growth and greater opacity, although the composition determined by X-rays was 100% hydroxylapatite.

The reason for increased opacity at higher temperatures may be the beginning of the decomposition of the hydroxylapatite [17]:

$$Ca_{10}(PO_4)_6(OH)_2 \rightarrow Ca_3(PO_4)_2 + Ca_4P_2O_9 + H_2O. \quad (2)$$

An indication of the formation of a second phase at the grain boundaries of another sample (F–33) fired at 1250° C for 1 h is shown in Fig. 8.

Direct transmission micrographs of sample C–6, thinned by ion bombardment, are shown in Figs. 9 and 10. They confirm the lack of pores and second phases deduced from the replica micrographs. Fig. 10 at high magnification shows no indication of a second phase or pores at the grain boundaries.

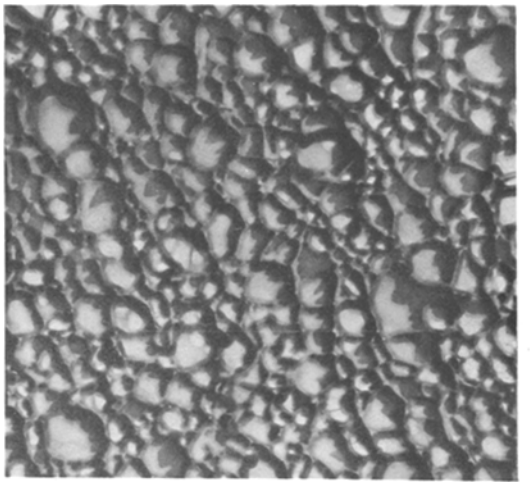

Figure 5 Electron micrograph from two-stage replica of hydroxylapatite fired 1 h at 1100° C (C–6), × 17 000.

Figure 6 Electron micrograph from two-stage replica of hydroxylapatite fired 1 h at 1150° C (C–8), × 17 500.

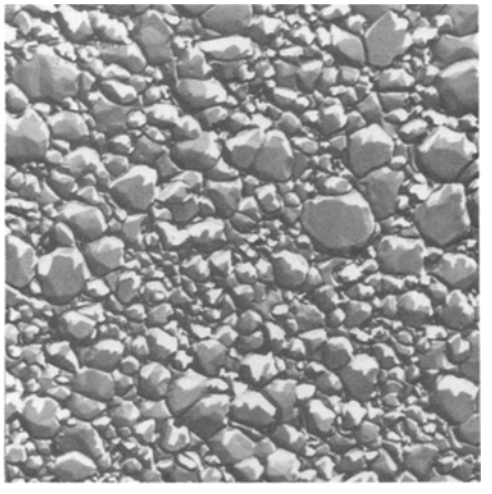

Figure 7 Electron micrograph from two-stage replica of hydroxylapatite fired 1 h at 1190° C (C–5), × 4 600.

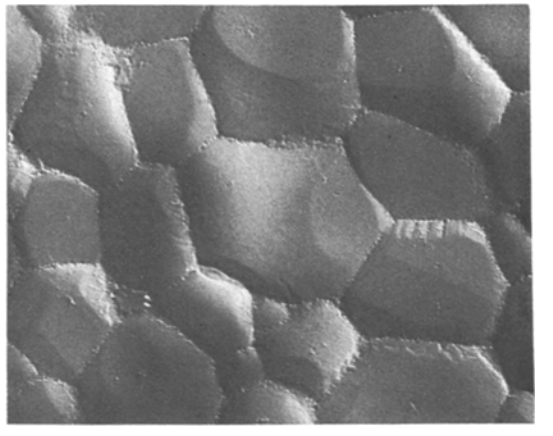

Figure 8 Electron micrograph from two-stage replica of hydroxylapatite fired 1 h at 1250° C (F–33), × 40 000.

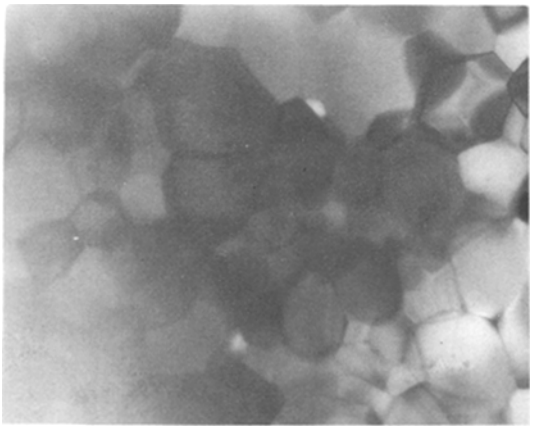

Figure 9 Direct transmission electron micrograph of ion-thinned hydroxylapatite fired at 1100° C for 1 h (C–6), × 144 000.

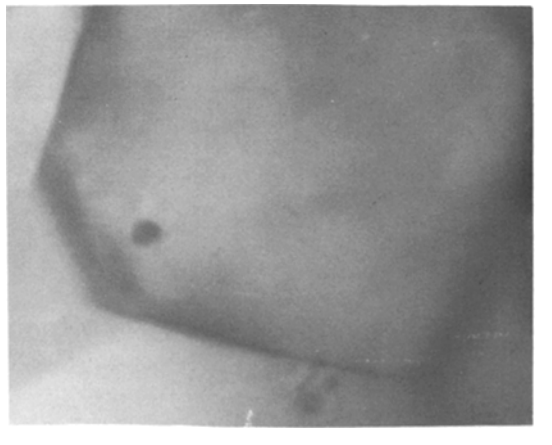

Figure 10 Direct transmission electron micrograph of ion-thinned hydroxylapatite fired at 1100° C for 1 h (C–6). Grain-boundary junction. The dark spot is an artefact of sample preparation, × 621 000.

Results of micrographic examination of other samples are also summarized in Table II. They show that starting with precipitated crystals that had not completely reacted to the hydroxylapatite stoichiometry, usually resulted in increased porosity, grain size, opacity, and reduced density.

From these results and those of the last section one can conclude that if pore-free, single-phase, translucent hydroxylapatite is desired the precipitated crystals must have reacted completely to the hydroxylapatite composition, and the optimum sintering temperature is 1100° C for a 1 h sintering time.

4.3. Strength

Fracture strengths of samples treated in different ways are listed in Table III. There was no statistically significant difference between the samples tested at 0.125 cm min^{-1} and 0.05 cm min^{-1}, or in four-point and three-point bending (Wilcoxen Rank Test). A statistically significant higher strength was found at liquid nitrogen temperature for samples N–54. The samples containing no β-whitlockite showed significantly higher strenghts as compared to those containing some second phase. A substantial increase in strength was found for polished samples, showing that damage introduced during cutting of the samples contributed significantly to their lower strengths.

The standard deviations in Table III were rather large and variable for as-cut samples becuase of the influence of sawing damage. Polished samples had a lower variation in strength as well as a higher strenght. The main factor in the strength is the surface condition of the sample.

The average compressive strength of sample C–6 was 917 MN m^{-2} (133 x 10^3 psi) ± 15% for 25 samples.

The average Knoop hardness of samples polished with 3 μm diamond paste was 480; and for samples polished in a gem tumbler was 489. The Knoop hardness of fused silica is about 560, and that of natural apatite is about 430.

4.4. Translucence

The opacity or translucence of a material can be characterized from its internal scattering and absorption. Hydroxylapatite shows no appreciable optical absorbance in the visible range, so opacity results from scattering from internal defects such as pores, second phases, and grain boundaries. The transclucence can be characterized by a scattering coefficient S, with units of cm^{-1} that does not depend on sample thickness [11]. From the theory of Kubelka and Munk [18, 19] this coefficent can be calculated from the total reflectance R_0 (diffuse plus specular) of a flat sampe of thickness d with a black backing from the equation:

$$S = \frac{R_0}{d(1-R_0)}. \quad (3)$$

R_0 must also be corrected for specular reflection at the sample surface. Values of S calculated in this way are included in Table II and have been discussed in Section 4.2.

4.5. Other properties

The electrical conductivity of the apatite was measured between about 250 and 450° C. Electrode polarization was marked, and at lower

TABLE III Fracture strength at 25° C of polycrystalline hydroxylapatite fired at 1100° C for 1 h at cross-head speed 0.125 cm min^{-1} three-point bending: samples as cut

Sample	wt% apatite from X-rays	Average fracture strength (MN m^{-2})(10^3 psi)	Standard deviations (MN m^{-2})	No. of samples	Remarks
N–54	87	78.6(11.4)	18.6	7	
N–54	87	71.0(10.3)	36.5	7	0.005 cm min^{-1} cross-head speed
N–54	87	101.3(14.7)	37.2	8	Tested in liquid N_2
N–53	87	84.1(12.2)	17.2	7	Four-point bending
N–54	87	160.0(23.2)	11.7	8	Polished with 600 grit alumina on two faces
N–30	100	195.8(28.4)	33.1	10	Polished down to 1 μm diamond on all four faces
E–9	60	80.0(11.6)	29.0	7	Fired at 1150° C
C–2	100	96.5(14.0)	20.7	7	Fired at 1000° C
C–6	100	111.7(16.2)	11.0	7	
D–8	100	97.9(14.2)	12.4	8	Fired at 1150° C

temperatures the measurements were unreliable because of the high resistance of the samples. An activation energy of about 30 kcal mol^{-1} was found, with a resistivity of about 4×10^9 Ωcm at 400° C. The results suggest that the conductivity is ionic, probably resulting from impurities.

The coefficient of thermal expansion was measured in the range 25 to 225° C and found to be 11×10^{-6} $°C^{-1}$.

Resistance to abrasion was measured on a grinder with a load of 447 g on 600 grit silicon carbide paper for 300 one-inch cycles. The weight loss for various materials in this test, in mg mm^{-2}, was: fused silica 0.10; 75% SiO_2–25% Na_2O glass 0.33; polycrystalline hydroxylapatite 1.17.

The modulus of elasticity in tension was measured to be about 34.5×10^9 N m^{-2} (5×10^6 psi).

5. Discussion

The present results agree well with previous studies of the precipitation of hydroxylapatite from alkaline aqueous solutions [16, 20, 21]. The first phase that precipitates, often called "amorphous" calcium phosphate, has a Ca/P ratio of 1.5 and is difficult to detect with X-rays [16, 21]. In the presence of sufficient additional calcium ion, this initial precipitate undergoes a slow maturation to produce X-ray detectable hydroxylapatite of correct stoichiometry [16]; in the absence of additional calcium, a calcium-deficient apatite is produced [22, 23]. Both "amorphous" calcium phosphate and calcium deficient hydroxylapatite serve as thermochemical precursors to the whitlockites [22, 23]. Thus the phase purity of the present polycrystalline hydroxylapatite is achieved by using precipitated hydroxylapatite of correct stoichiometry. In contrast, in some previously reported studies on sintered hydroxylapatite, commercial "hydroxylapatites" from various sources were found to produce ceramics containing variable mixtures of hydroxylapatite and whitlockite [3, 5].

There is considerable grain growth druing sintering even at a firing temperature of 1000° C, since the initial particle size is about 200 Å, whereas the grain size in the material sintered at 1000° C is 1500 Å. At higher temperature grain growth continues at an accelerated rate. The grain size d is often given by [24, 25]:

$$d = Kt^n$$

when n is usually between 1/3 and 1/2. The activation energy for grain growth can be found from a plot of log d against $1/T$ for a constant sintering time. Such a plot is shown in Fig. 11 for the data in Table II, and gives an activation energy for grain growth in hydroxylapatite of about 56 kcal mol^{-1}. This activation energy is similar to that for the diffusion of oxygen in many different oxides [26], and it is possible that the rate of grain growth in apatite is related to diffusional processes in the apatite.

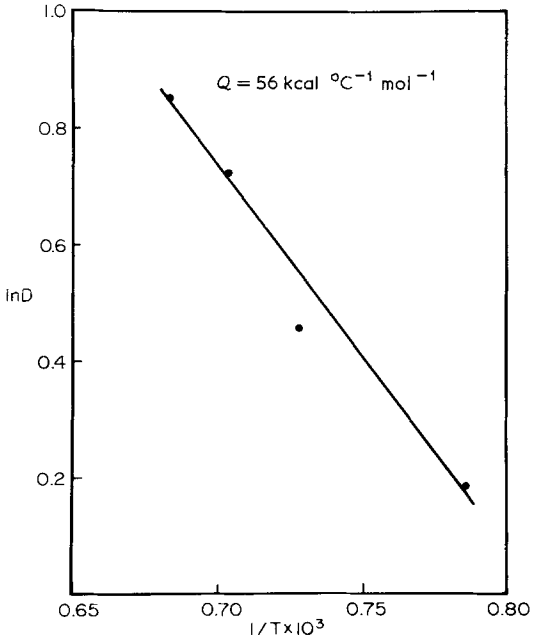

Figure 11 Log grain size versus reciprocal firing temperature for polycrystalline hydroxylapatite.

The present polycrystalline hydroxylapatite is much stronger than previously reported hydroxylapatites [4, 5] that were made by sintering pressed powders. The compressive strengths of these materials (207 to 275 MN m^{-2}, 30 to 40×10^3 psi) were only about one-third or less the compressive strength of the present material, and presumably a similar disparity exists in tensile strenghts, although these were not reported for the other materials. This mechanical superiority results both from the high purity of the starting hydroxylapatite and from the special forming process. During the drying of the precipitated hydroxyapatite the crystals compact like clay to produce a green state that is devoid of the pore-producing aggregates normally present in compacts prepared from dried powders [27]. These dried crystals

contain about 6% water, which is probably absorbed on the crystal surfaces and bonds them together. As the crystals are heated during the firing process, most of this water is driven off before sintering begins at 900 to 1000° C. The lack of fine pores in the fired samples probably results from a combination of the very small initial particle size and the absence of particle aggregates. This absence of pores, coupled with the absence of second phases, results in a polycrysatlline hydroxylapatite with superior optical and mechanical properties.

References

1. E. B. NERY, K. L. LYNCH, W. M. HIRTHE and K. H. MUELLER, *J. Periodontol.* **46** (1975) 328.
2. M. JARCHO, K. I. GUMAER, J. F. KAY and R. H. DOREMUS, to be published.
3. E. A. MONROE, W. VOTAVA, D. B. BASS and J. MCMULLERS, *J. Dent. Res.* **50** (1971) 860.
4. W. R. RAO and R. F. BOEHM, *ibid* **53** (1974) 1351.
5. W. HUBBARD, Ph. D. thesis, Marquette University (1974).
6. D. M. ROY and S. K. LINNEHAN, *Nature* **247** (1974) 221.
7. M. JARCHO, U.S. and Foreign Patent Applications filed.
8. M. D. FRANCIS, J. A. GRAY and W. J. GRIEBSTEIN, *Adc. Oral Biol.* **3** (1968) 83.
9. J. E. HILLIARD, *Metal Prog.* May (1964) 99.
10. J. E. HILLIARD and J. W. CAHN, "Evalutation of Procedures in Quantitative Mettalography for Volume Fraction Analysis", *Trans. Met. Soc. AIME* **221** (1961) 344.
11. M. B. THOMAS and R. H. DOREMUS, *J. Amer. Ceram. Soc.* **56** (1976) 229.
12. J. BOBICK, M. S. Thesis, Rensselaer Polytechnic Institute, Troy, New York (1976).
13. J. MURPHY and J. RILEY, *Anal. Chem. Acta.* **27** (1962) 31.
14. E. HAYCK and H. NEWESELY, *Inorg. Synthesis* **7** (1963) 63.
15. B. D. CULLITY, "Elements of X-ray Diffraction" (Addison-Wesley, Reading, Mass, 1967) p. 388.
16. E. D. EANES, J. H. GILLESSEN and A. L. POSNER, *Nature* **208** (1965) 365.
17. T. R. N. KUTTY, *Ind. J. Chem.* **11** (1973) 695.
18. P. KUBELKA and F. MUNK, *Z. Tech. Physik.* **12** (1931) 593.
19. G. KORTUM, "Reflectance Spectroscopy" (Springer-Verlag, New York, 1969) p. 103.
20. G. H. NANCOLLAS and B. TOMAZIC, *J. Phys. Chem.* **78** (1974) 2218.
21. A. S. POSNER and F. BETTS, *Accounts Chem. Res.* **8** (1975) 273.
22. J. A. S. BETT, L. G. CHRISNER and W. K. HALL, *J. Amer. Chem. Soc.* **89** (1967) 5535.
23. E. D. EANES, *Calc. Tiss. Res.* **5** (1970) 123.
24. R. L. COBLE, *J. Appl. Phys.* **32** (1961) 787.
25. K. W. LAY, in "Materials Research", Vol. 6 edited by G. C. KUCZYNSKI (Plenum, New York, 1972) p. 65.
26. D. KINGERY, "Introduction to Cermaics" (Wiley, New York, 1960) p. 232.
27. J. E. BURKE, and J. H. ROSOLOWSKI, General Electrical Technical Information Series, Report No. 73CRD268, 1973.

Received 15 March and accepted 5 April 1976.